CONF-900764--4

LBL-28244

Center for Advanced Materials

CAM

Presented at the Fourth International Conference on Fatigue and Fatigue Thresholds, Honolulu, HI, July 15–20, 1990, and to be published in the Proceedings

On the Micromechanisms of Fatigue-Crack Propagation in Aluminum-Lithium Alloys: Sheet vs. Plate Material

K.T. Venkateswara Rao, R.J. Bucci, and R.O. Ritchie

December 1989

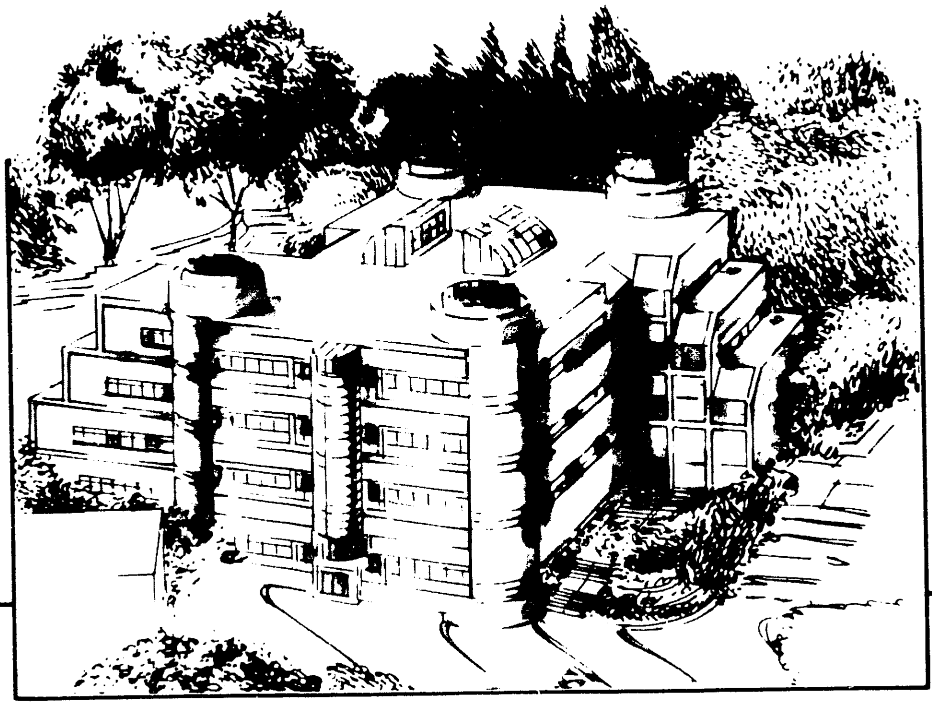

Materials and Chemical Sciences Division

Lawrence Berkeley Laboratory • University of California

ONE CYCLOTRON ROAD, BERKELEY, CA 94720 • (415) 486-4755

Prepared for the U.S. Department of Energy under Contract DE-AC03-76SF00098

LBL--28244

DE92 000926

ON THE MICROMECHANISMS OF FATIGUE-CRACK PROPAGATION IN ALUMINUM-LITHIUM ALLOYS: SHEET vs. PLATE MATERIAL

K. T. Venkateswara Rao,† R. J. Bucci* and R. O. Ritchie†

†Center for Advanced Materials, Materials and Chemical Sciences Division,
Lawrence Berkeley Laboratory
and
Department of Materials Science and Mineral Engineering
University of California, Berkeley, CA 94720

*Alcoa Laboratories, Alcoa Center, Pittsburgh, PA 15069

December 1989

Published in *FATIGUE 90, Proceedings of the Fourth International Conference on Fatigue and Fatigue Thresholds*, Honolulu, Hawaii, H. Kitagawa and T. Tanaka, eds.

Work supported by the Director, Office of Energy Research, Office of Basic Energy Sciences, Materials Sciences Division of the U.S. Department of Energy under Contract No. DE-AC03-76SF00098.

ON THE MICROMECHANISMS OF FATIGUE-CRACK PROPAGATION IN ALUMINUM-LITHIUM ALLOYS: SHEET vs. PLATE MATERIAL

K. T. Venkateswara Rao†, R. J. Bucci* and R. O. Ritchie†

Micromechanisms influencing the propagation of long (> 10 mm) fatigue cracks in aluminum-lithium alloys are examined by specifically comparing crack-growth kinetics in a peak-aged Al-Li-Cu-Zr alloy 2090, processed as 1.6-mm thin (T83) sheet and 12.7-mm thick (T81) plate. It is found that in general crack-growth rates are significantly faster in the sheet material at equivalent stress-intensity levels, due to differences in the role of crack-tip shielding, resulting from crack deflection and consequent crack closure from wedging of fracture-surface asperities. Microstructurally, such differences are related to variations in the degree of recrystallization, grain structure and deformation texture in the two wrought-product forms.

INTRODUCTION

Aluminum-lithium alloys constitute a new generation of low-density, high-strength and high-stiffness aerospace materials, which have been developed primarily to replace 2000 and 7000 series aluminum alloys used in existing aircraft structures. Compared to such traditional alloys, Al-Li alloys exhibit remarkably superior (long) fatigue-crack propagation resistance (1-7). These superior fatigue properties were originally thought to be associated with the higher elastic modulus of these materials, which reduces crack-tip opening displacements, and with greater planarity of slip arising from the shearable nature of the coherent, ordered strengthening precipitates, e.g., δ' Al_3Li (1,2). Recent studies (3-7), however, have indicated that the effect is principally associated with enhanced crack-tip shielding, where the near-tip crack-driving force is locally reduced by microstructurally-induced crack-path deflection and resultant crack-closure mechanisms.

Such reports of the superior crack-growth resistance of Al-Li alloys have been largely based on results on wrought thick-section plate, where microstructures are generally unrecrystallized, anisotropic and strongly textured, all factors which promote crack-path deflection, and consequently higher shielding levels, in specific orientations. However, in sheet material where microstructures are partially recrystallized and more isotropic, such superior fatigue-crack growth resistance may be compromised. It is therefore the intent of the present paper to examine the effect of wrought-product form on the resistance to (long-crack) fatigue-crack propagation in a commercial Al-Li-Cu-Zr alloy 2090-T8, and compare results with those in a traditional Al-Zn-Cu-Mg alloy 7075-T6.

†Center for Advanced Materials, Lawrence Berkeley Laboratory and Department of Materials Science and Mineral Engineering, University of California, Berkeley, CA 94720.
*Alcoa Laboratories, Alcoa Center, Pittsburgh, PA 15069.

EXPERIMENTAL PROCEDURES

Ingot metallurgy (I/M) Al-2.05Li-2.86Cu-0.12Zr (wt.%) alloy 2090, in the form of 1.6-mm thin sheet and 12.7-mm thick plate, was provided in the solution treated, stretched and near peak-aged condition. Processing procedures differ slightly for thin (<4 mm) sheet and plate and are designated as T83 and T81 tempers respectively; details are described elsewhere (5,7). Grain structures in sheet material show evidence of continuous recrystallization, with an equiaxed 20 to 30 μm grain size; in contrast, coarse, unrecrystallized and pan-cake shaped (2 mm x 0.5 mm x 50 μm) grains are characteristic of plate material (Fig. 1). Both sheet and plate material, however, are hardened in the matrix by coherent δ' spherical precipitates, θ'-like (Al_2Cu) and T_1 (Al_2CuLi) plates, and β' (Al_3Zr) dispersoids, with some degree of grain-boundary precipitation resulting, respectively, in 100 and 50 nm-wide δ'-precipitate-free zones. Mechanical properties are listed in Table 1.

TABLE 1 - Room Temperature Mechanical Properties of 2090-T8 Alloy

Product Form	Yield Strength σ_y (MPa)	UTS (MPa)	% Elongation (on 25 mm)	Fracture Toughness K_c (MPa$\sqrt{m}$)
1.6-mm sheet	505	568	6.8	43 (L-T)
12.7-mm plate	552	589	9.3	36 (L-T)

Fatigue-crack growth tests were performed in moist room temperature air (22°C, 45% relative humidity) on automated servo-hydraulic testing machines operating at a frequency of 50 Hz (sine wave) with load ratios ($R = K_{min}/K_{max}$) of 0.1 and 0.75 using compact tension specimens machined in the L-T orientation. Crack length and crack closure were continuously monitored *in situ* using d.c. electrical-potential and back-face strain compliance techniques, respectively; the latter measurements involved determining the closure stress intensity, K_{cl}, at first contact of the fracture surfaces during unloading (5,8).

Fracture surfaces were examined using scanning electron microscopy. In addition, metallographic sections of the crack path, both perpendicular and parallel to the crack-advance direction, were imaged optically; parallel sections were taken at the specimen mid-thickness.

RESULTS

The variation in (long-crack) fatigue-crack propagation rates and corresponding crack-closure behavior (R = 0.1) for sheet and plate Al-Li alloy 2090-T8 are plotted in Fig. 2 as a function of the nominal stress-intensity range, $\Delta K = K_{max} - K_{min}$; corresponding results for alloy 7075-T6 (Al-6.1Zn-2.3Cu-2.2Mg, wt.%) are shown for comparison. Several points are worthy of note. First, fatigue cracks in the Al-Li alloy grow up to 2 to 3 orders of magnitude faster in T83 sheet compared to T81 plate, particularly as ΔK levels approach the fatigue threshold, ΔK_{TH}. In contrast, the traditional 7075-T6 alloy shows no such differences between sheet and plate, at least for ΔK levels below ~20 MPa$\sqrt{m}$. Second, consistent with the higher growth rates in the 2090-T83 sheet, measured crack-closure levels are significantly lower than in the T81 plate. Third, the 2090-T8 Al-Li alloy, both as sheet and plate, displays generally superior fatigue-crack growth resistance compared to corresponding 7075-T6 alloys, except at near-threshold levels in sheet materials where behavior is similar.

Fractographically, the higher growth rates and lower closure levels in Al-Li alloy sheet are associated with essentially linear crack-paths and relatively flat transgranular-shear fracture surfaces. The plate material, conversely, exhibits highly deflected and meandering crack profiles, both along the crack-growth direction and through the specimen thickness, consistent with higher closure levels (Fig. 3). Such crack advance proceeds along {111} slip bands (6,9) due to the shearable nature of coherent δ' precipitates and pronounced texture in plate, resulting in a rough fracture-surface topography covered with large transgranular-shear facets (Fig. 3f). No distinct changes in these fracture morphologies were apparent in either product form over the range of growth rates investigated.

The influence of load ratio on Al-Li alloy sheet and plate is shown in Fig. 4. Similar to most I/M alloys, higher load ratios induce faster growth rates, particularly at near-threshold levels. The effect is particularly pronounced in 2090-T81 plate where closure levels are especially high at $R = 0.1$, presumably due to crack wedging by the enlarged fracture-surface asperities (roughness-induced closure). With increasing R, the larger crack-tip opening displacements act to minimize such shielding, such that at $R = 0.75$, differences in crack-growth behavior between sheet and plate material are less apparent.

DISCUSSION

Reports (e.g., 10-13) on the effect of specimen thickness on fatigue-crack propagation in metallic alloys are generally conflicting. Increasing thickness has been found to accelerate, retard or have no effect on crack-growth rates; differences in behavior have been attributed to variations in fracture mode (Mode I vs II or III) and stress state (plane stress vs plane strain), the onset of general yielding, changes in fracture mechanism, and crack-closure effects. For example, higher growth rates observed in thick sections can be due to inherently faster crack advance under plane-strain conditions, induced by lower (plasticity-induced) crack-closure levels (10) and an increased contribution from fast-fracture ("static") modes (11,12) triggered by the triaxial stress state. Conversely, rapid crack extension in thin sheets may be induced by larger plastic zone and specimen-geometry effects (11,13) which promote stress relaxation and the earlier onset of ~45° slant fracture. These explanations, however, pertain primarily to high growth-rate behavior; at lower ΔK levels, they are less relevant as crack-tip deformation conditions approach that of plane strain for most thicknesses.

In the present study, deformation conditions in both sheet and plate 2090-T8 at R =0.1 are predominantly plane strain up to ΔK levels of ~ 25 MPa$\sqrt{}$m, as maximum plastic-zones ($\approx 1/2\pi[K_{max}/\sigma_y]2$) and shear-lip sizes do not exceed 6% of the thickness in the sheet material. Morever, no evidence of "static" fracture modes is apparent in either product form over the entire spectrum of growth rates. However, it *is* clear that crack-closure levels are significantly higher in plate material. Accordingly, we conclude that the observed differences in fatigue-crack growth behavior between sheet and plate 2090-T8 are principally associated with variations in crack-path deflection and resulting crack closure from the wedging of fracture-surface asperities (6). As shown in Fig. 3b, marked slip planarity and pronounced deformation texture in the T81 plate results in highly faceted, crystallographic crack growth along intersecting slip bands; the accompanying crack deflection is additionally promoted through the majority of the specimen thickness and induces sharp facets with an included angle of $\sim 60°$ from the intersection of {111} slip planes (9). These effects, together with the coarse, unrecrystallized grain structure and weak short-transverse properties of the T81 plate, provide the principal sources of high shielding levels and hence reduced crack-propagation rates. Such significant shielding effects are not prominent in the T83 sheet material because the finer, recrystallized grain structure and reduced texture induce a more linear crack path and hence faster crack-propagation rates. However, *it should be noted even without large contributions from crack closure, Al-Li sheet material still displays better crack-growth resistance than traditional alloys*, particularly at higher growth rates, presumably due to the beneficial role of planar-slip deformation in promoting reversibility of slip at the crack tip.

CONCLUSIONS

Based on a study of the fatigue-crack growth behavior of long cracks (> 10 mm) in peak-aged Al-Li-Cu-Zr alloy 2090-T8, processed in the form of 1.6-mm thin sheet and 12.7-mm thick plate, the following conclusions can be made:

1. Fatigue-crack propagation rates in Al-Li alloy 2090-T8 at a load ratio R of 0.1 are found to be 2 to 3 orders of magnitude faster in T83 sheet, compared to T81 plate at equivalent stress-intensity levels. The effect is most pronounced at near-threshold levels and least pronounced at R = 0.75. No such differences in sheet and plate material are seen for traditional 7075-T6 alloys.

2. Such differences in the crack-growth behavior of 2090-T8 sheet and plate material are attributed primarily to microstructurally-induced differences in crack-tip shielding. In plate material,

where the microstructure is unrecrystallized and shows coarse elongated grains with strong deformation texture, fatigue-crack paths are unusually tortuous with significant crack deflection; such a morphology promotes marked (roughness-induced) crack closure, concomitant with reduced crack-growth rates. In sheet material, conversely, microstructures are recrystallized with a finer and essentially equiaxed grain size; crack paths are correspondingly highly linear with the result that crack-closure levels are significantly reduced.

Acknowledgements: This work was supported by the Director, Office of Basic Energy Sciences, Materials Sciences Division of the U.S. Department of Energy under Contract No. DE-ACO3-76SF00098 (for KTVR and ROR), and by the Department of the Navy, Naval Surface Warfare Center, under Contract No. N60921-84-C-0078 (for RJB).

REFERENCES

(1) Coyne, E. J., Sanders, T. H. and Starke, E. A., in *"Aluminum-Lithium Alloys"*, T. H. Sanders and E. A. Starke (eds.), TMS-AIME, Warrendale, PA, 1981, pp. 293-305.

(2) Harris, S. J., Noble, B., Dinsdale, K., in *"Aluminum-Lithium Alloys II"*, T. H. Sanders and E. A. Starke (eds.), TMS-AIME, Warrendale, PA, 1983, pp. 219-33.

(3) Vasudévan, A. K., Bretz, P. E., Miller, A. C. and Suresh, S., *Mater. Sci. Eng.*, Vol. 64, 1984, pp. 113-22.

(4) Jata, K. V. and Starke, E. A., *Metall. Trans. A*, Vol. 17A, 1986, pp. 1011-26.

(5) Venkateswara Rao, K. T., Yu, W. and Ritchie, R. O., *Metall. Trans. A*, Vol. 19A, 1988, pp. 549-61.

(6) Venkateswara Rao, K. T., Piascik, R. S., Gangloff, R. P. and Ritchie, R. O., in *"Aluminum-Lithium Alloys"*, T. H. Sanders and E. A. Starke (eds.), Vol. II, MACE Publ. Ltd., Birmingham, U.K., 1989, pp. 955-71.

(7) Bucci, R. J., Malcolm, R. C., Colvin, E. L., Murtha, S. and James, R. S., Final Report, Naval Air Development Center, Warminster, PA, Contract. No. N60921-84-C-0078, 1989.

(8) Ritchie, R. O. and Yu, W., in *"Small Fatigue Cracks"*, R. O. Ritchie and J. Lankford (eds.), TMS-AIME, Warrendale, PA, 1986, pp. 167-89.

(9) Yoder, G. R., Pao, P. S., Imam, M. A. and Cooley, L. A., *Scripta Metall.*, Vol. 22, 1988, pp. 1241-44.

(10) Lindley, T. C. and Richards, C. E., *Mater. Sci. Eng.*, Vol. 14, 1974, pp. 281-93.

(11) Ritchie, R. O., Smith, R. F. and Knott, J. F., *Metal Sci.*, Vol. 9, 1975, pp. 485-92.

(12) Griffiths, J. R. and Richards, C. E., *Mater. Sci. Eng.*, Vol. 11, 1973, pp. 305-10.

(13) Jack, A. R. and Price, A. T., *Acta Metall.*, Vol. 20, 1972, pp. 857-66.

(14) Bretz, P. E., Vasudévan, A. K., Bucci, R. J. and Malcolm, R. C., Final Report, Naval Air Systems Command, Washington, Contract No. N00019-79-C-0258, 1981.

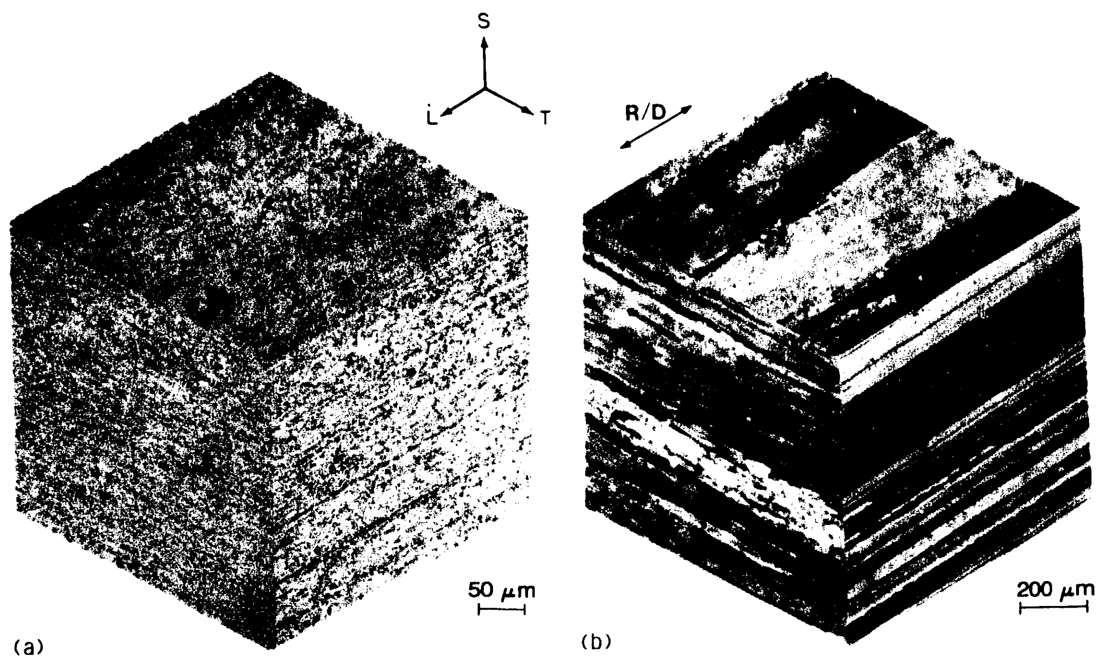

XBB 8912-10552-A

Figure 1. Three dimensional optical micrographs of grain structures in a) T83 sheet and b) T81 plate of Al-Li alloy 2090.

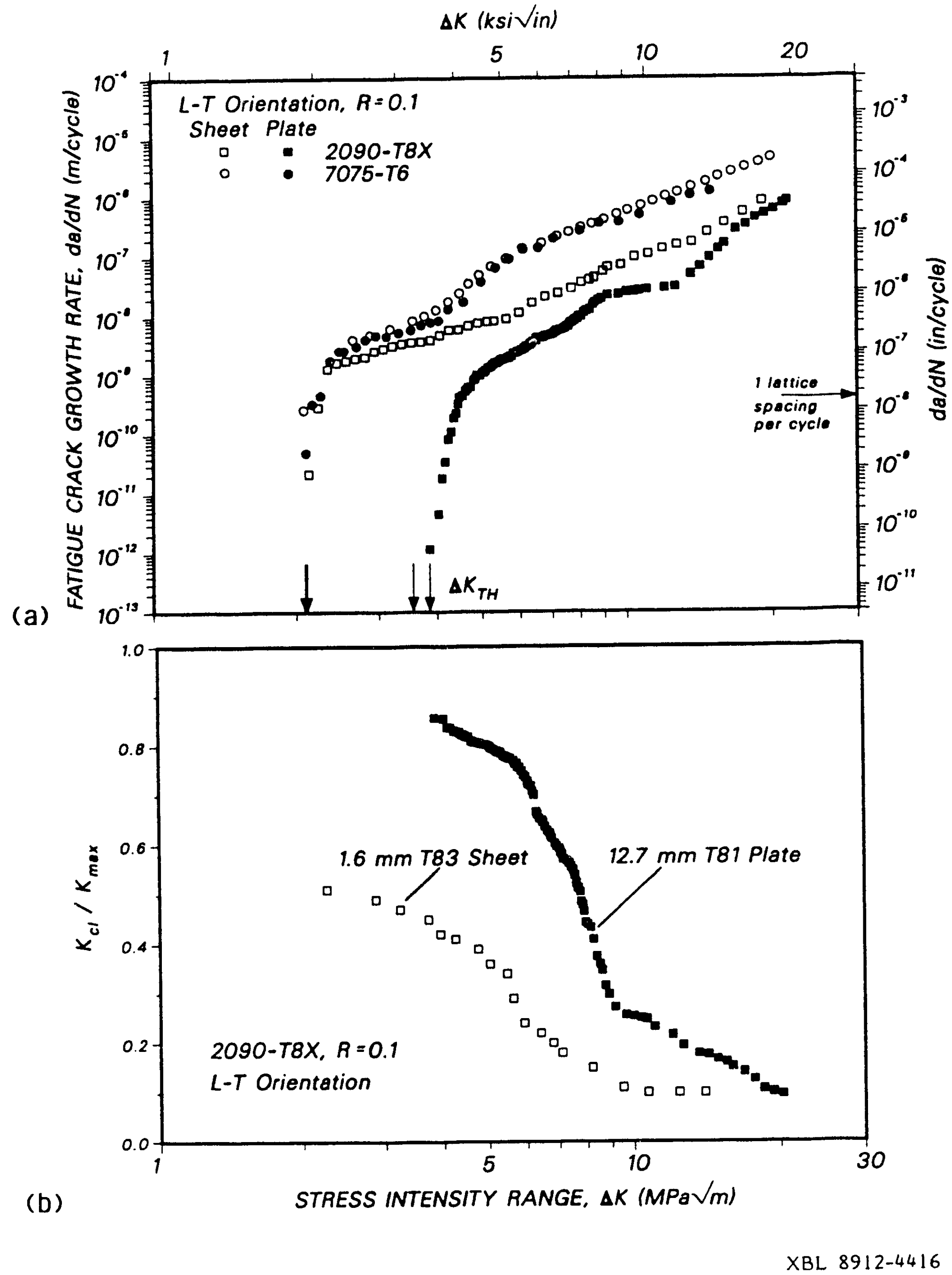

Figure 2. a) Fatigue-crack growth and b) crack-closure (K_{cl}/K_{max}) behavior in 2090-T8 sheet and plate at R = 0.1, as a function of the nominal stress-intensity range ΔK. Growth-rate data are compared with corresponding results on 7075-T6 (7,14). T81 plate data obtained on 6.4 mm thick specimens (T/2 location).

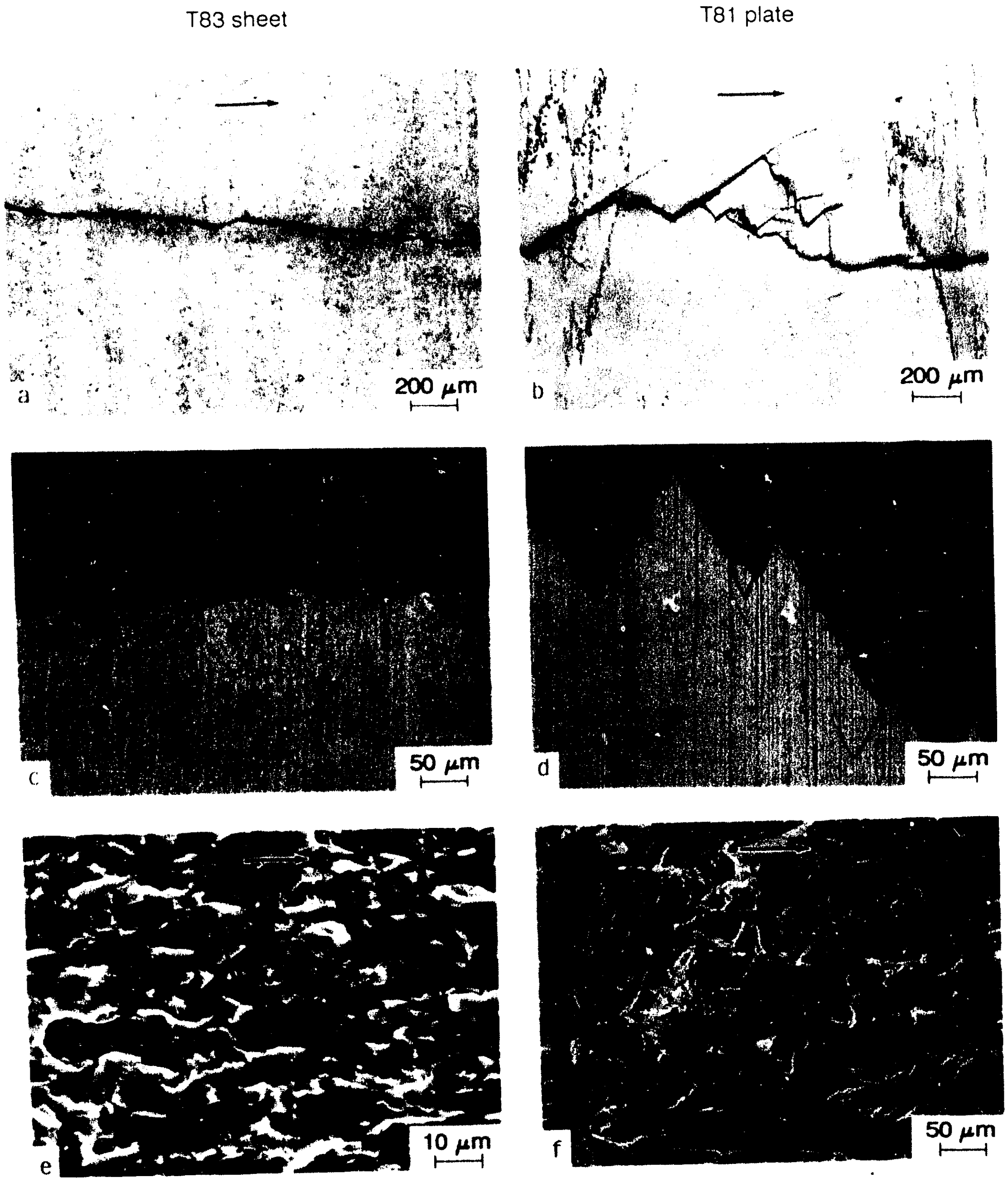

XBB 8912-10708

Figure 3. Comparison of fatigue-crack path and fracture-surface morphologies in 2090-T8 Al-Li alloy as T81 (plate) and T83 (sheet), showing (a,b) crack paths along the crack-growth direction (c,d) crack paths across the specimen thickness, and (e,f) fracture surfaces. Arrows indicate general direction of crack growth.

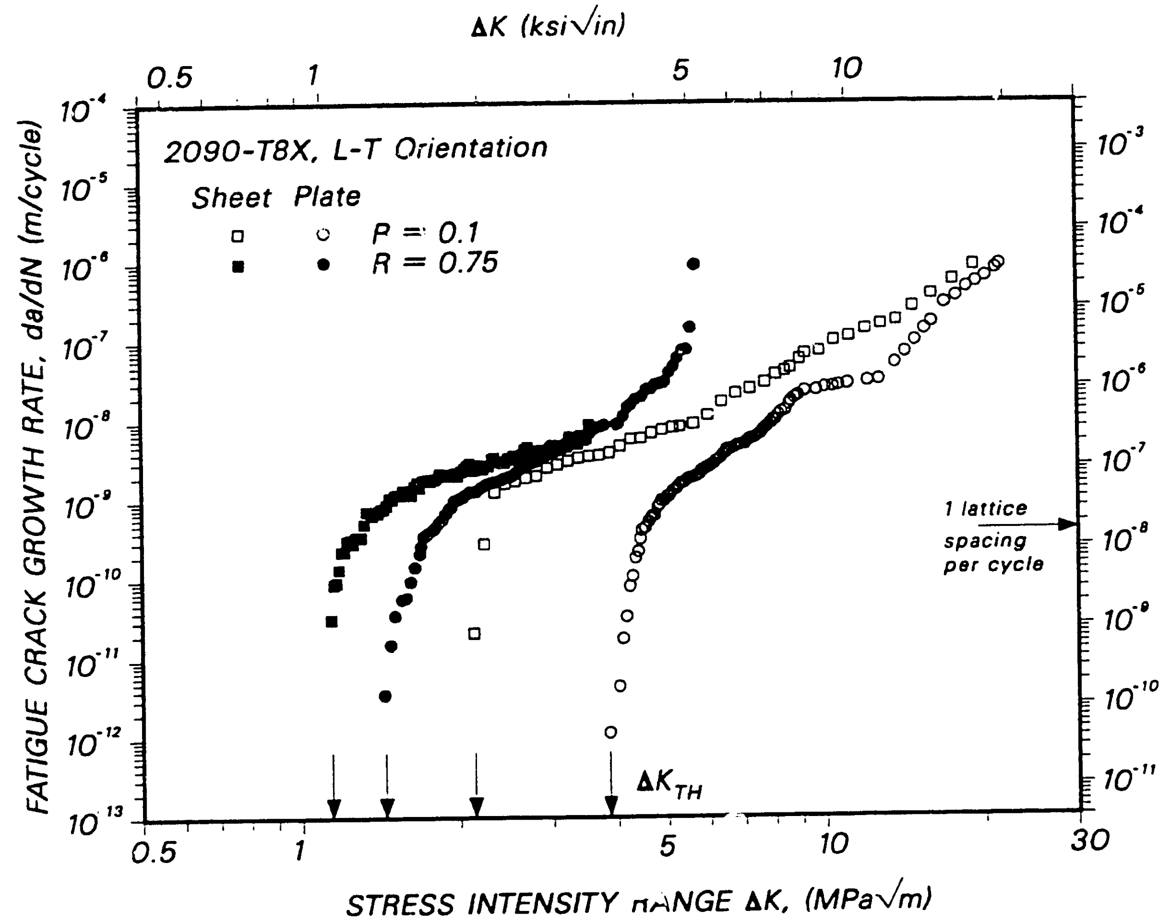

XBL 8912-4417

Figure 4. Influence of load ratio, $R = K_{min}/K_{max}$, on fatigue-crack growth rates in peak-aged 2090-T8 sheet and plate material.

END

DATE FILMED

11 / 06 / 91